Paper 182

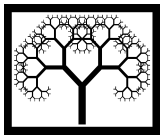

Proceedings of the Eleventh International Conference
on Computational Structures Technology,
B.H.V. Topping, (Editor),
Civil-Comp Press, Stirlingshire, Scotland

Axisymmetric Large Deflection Analysis of an Annular Circular Plate subject to Rotational Symmetric Loading

M. Altekin and R.F. Yükseler
Department of Civil Engineering
Yildiz Technical University, Esenler, Istanbul, Turkey

Abstract

This computational paper presents the geometrically nonlinear bending analysis of a circular plate with a concentric circular hole. Axisymmetric transverse load is considered in the study. The analysis is made for several boundary conditions including simply supported edge (S), or clamped edge (C), or free edge (F). The thickness of the plate is considered to be uniform. The material is assumed to be isotropic and homogeneous. The accuracy of the results is verified by checking the unknowns with those available in the literature. The influence of the geometrical parameters on the displacements and the stress resultants are investigated by sensitivity analysis.

Keywords: large deflection, circular plate, annular, bending, axisymmetric, nonlinear.

1 Introduction

Analysis of plates has always been a challenging topic and has received significant attention of researchers [1-8]. The current work is motivated by the scarcity of contributions on the geometrically nonlinear bending analysis of annular circular plates. Large deflection of a uniform annular circular plate under axisymmetric transverse load is studied numerically in this study. Geometrically nonlinear shallow spherical shell equations [1] are used in the paper. Transverse shear deformation is not considered in these equations. The formulation is based on reorganizing and rearranging the governing equations some of which are coupled equations, presented in reference [1]. Since an axisymmetric plate under rotational symmetric loading is investigated, the system of partial differential equations is automatically transformed into a system of ordinary differential equations which are solved numerically by the finite difference and the Newton-Raphson methods, respectively. Total number of points to be used along the radial coordinate is determined by performing

convergence studies. Six unknowns at each point are defined in the solution. The unknowns are chosen to be the deflection, the radial displacement, the rotation, the membrane force, the transverse shear force, and the bending moment. Firstly, the differential equations are converted into algebraic equations by the finite difference method. Forward, backward, and central finite difference formulas of $O\left(h^2\right)$ are employed. Next, the Newton-Raphson method is used to find the unknowns. The boundary conditions along the inner and the outer edge of the plate are satisfied exactly. The present paper is a complementary study of the work done by Altekin and Yükseler [2]. The main advantage of the formulation used in the current paper is that only one of the six equations is in coupled form. Six unknowns are considered at each grid point along the radial coordinate. The influence of the plate thickness on the displacement components and the stress resultants is investigated by sensitivity analysis. Several values of α is considered for the numerical examples.

2 Formulation

2.1 Basic Equations

First, due to the radial symmetry of the plate and the loading, the geometrically nonlinear ordinary differential shallow spherical shell equations are reorganized in terms of three displacement components (w,u,β), and three stress resultants (n_r,q_r,m_r). Next, the height of the shallow spherical shell is set to zero in the current study and a circular plate of radius a is obtained. Therefore,

$$m_r + r\,m_r{}' + D\left(\frac{w'}{r} + \nu\,\beta'\right) - r\,q_r = 0 \tag{1}$$

$$\left(1-\nu\right)n_r + r\,n_r{}' - E\,t\,\frac{u}{r} = 0 \tag{2}$$

$$q_r + r\,q_r{}' + r\,\beta'\,n_r + \frac{E\,t}{r}w'u + \nu\,w'\,n_r + r\,q = 0 \tag{3}$$

$$m_r + D\,\beta' + D\frac{\nu}{r}\beta = 0 \tag{4}$$

$$u' + \frac{1}{2}\beta^2 - \frac{\left(1-\nu^2\right)}{E\,t}n_r + \nu\frac{u}{r} = 0 \tag{5}$$

$$w' - \beta = 0 \tag{6}$$

are obtained where $(\ )' = \dfrac{d(\ )}{dr}$.

Here, w,u,β are the deflection, the radial displacement and the rotation, respectively. The symbols denoted by r,ν,E,t are the radial coordinate, the

Poisson's ratio, the Young's modulus, and the thickness of the plate, respectively. The stress resultants n_r, q_r, m_r are the membrane force, the transverse shear, and the bending moment, respectively. The uniform external pressure is introduced by $q(r) = q$. The non-dimensional parameters defined as upper-case letters (W, U, Q, N_r, Q_r, M_r) are introduced by

$$w = Wt, \quad u = Ut, \quad r = \xi a, \quad c = \frac{a}{t}, \quad D = \frac{Et^3}{12(1-\nu^2)}, \quad \alpha = \frac{b}{a} \tag{7}$$

$$q = QE, \quad n_r = EtN_r, \quad q_r = EtQ_r, \quad m_r = Et^2 M_r \tag{8}$$

where D is the bending rigidity of the plate, and b is the radius of the circular hole. Hence, α represents the parameter of hole and stands for the ratio of the inner radius to the outer radius. The parameter of thickness is denoted by c. Substituting the non-dimensional variables into Equations (1-6), we have the ordinary differential operators $L_1, L_2, L_3, L_4, L_5, L_6$ given by

$$L_1 = (1-\nu^2)M_r + (1-\nu^2)\xi\frac{dM_r}{d\xi} + \frac{1}{12c^2\xi}\frac{dW}{d\xi} + \frac{\nu}{12c}\frac{d\beta}{d\xi} - (1-\nu^2)c\xi Q_r = 0 \tag{9}$$

$$L_2 = (1-\nu)N_r + \xi\frac{dN_r}{d\xi} - \frac{1}{c\xi}U = 0 \tag{10}$$

$$L_3 = Q_r + \xi\frac{dQ_r}{d\xi} + \xi\frac{d\beta}{d\xi}N_r + \frac{1}{c^2\xi}\frac{dW}{d\xi}U + \frac{\nu}{c}\frac{dW}{d\xi}N_r + c\xi Q = 0 \tag{11}$$

$$L_4 = 12(1-\nu^2)cM_r + \frac{d\beta}{d\xi} + \frac{\nu}{\xi}\beta = 0 \tag{12}$$

$$L_5 = \frac{1}{c}\frac{dU}{d\xi} + \frac{1}{2}\beta^2 - (1-\nu^2)N_r + \frac{\nu}{c\xi}U = 0 \tag{13}$$

$$L_6 = \frac{1}{c}\frac{dW}{d\xi} - \beta = 0 \tag{14}$$

Equations (9-14) are converted to algebraic equations via the finite difference method using the forward, central and backward differences, and then they are solved by the Newton-Raphson method. The grid points are located along the radial coordinate and six unknowns $(W, U, \beta, N_r, Q_r, M_r)$ are defined at each point.

2.2 Boundary Conditions

The boundary conditions to be satisfied exactly in the study are

- at the clamped edge (C): $W = U = \beta = 0$,
- at the simply supported edge (S): $W = U = M_r = 0$,
- at the free edge (F): $N_r = Q_r = M_r = 0$.

3 Numerical Results

Convergence studies reveal that 81 grid points along the radial coordinate are sufficient for admissible accuracy where the first grid point is located at the plate perimeter (i.e., for $\xi = 1$), and the last one is at the center (i.e., for $\xi = 0$) of the plate (Table 1). Accuracy of the results is checked by comparing the deflections at a given point (i.e., W^*_{mid} is computed for $\xi = 0.55$, and $W^*_{\max}$ is computed for $\xi = 1$) for two different types of transverse loads (i.e., uniform pressure or linearly varying axisymmetric load) with those available in the literature (Table 2). The boundary conditions of the annular plate are identified by two upper-case letter symbols [8]. For example, C-F denotes an annular plate with a clamped inner edge (C), and a free outer edge (F).

The numerical parameters used in the paper are

$$a = 1\ m, \qquad E = 2\times 10^6\ N/m^2, \qquad \nu = 0.3, \qquad 0.1 \le \alpha \le 0.8 \qquad (15)$$

where a and b are the outer and inner radius, respectively.

$q(r) = q, \quad Q = 1\times 10^{-8}, \quad c = 100$	$W_{\max}$		$W_{\max}$
Number of grid points (n)	$\alpha = 0.1$		$\alpha = 0.4$
$n = 41$	0.0190		0.0037
$n = 51$	0.0191		0.0037
$n = 81$	0.0191		0.0037
$n = 101$	0.0192		0.0037

Table 1. Convergence study for $W_{\max}$ of a C-C plate under uniform pressure

$W^* = \frac{wD}{qa^4}$		Boundary conditions		Load	c
9.1239×10^{-4}		C-C plate	W^*_{mid}	$q(r) = q\frac{(r-b)}{(a-b)}$	$c = 100$
9.1239×10^{-4}		C-C plate			$c = 200$
9.1322×10^{-4} [8]		C-C plate			$c = 1000$
0.0040		C-S plate	W^*_{mid}	$q(r) = q$	$c = 100$
0.0040		C-S plate			$c = 200$
0.0040 [8]		C-S plate			$c = 1000$
0.0755		C-F plate	$W^*_{\max}$	$q(r) = q$	$c = 100$
0.0751		C-F plate			$c = 200$
0.0757 [8]		C-F plate			$c = 1000$

Table 2. Comparison of the results ($\alpha = 0.1,\ \xi = 0.55,\ \nu = 0.3,\ Q = 1\times 10^{-10},\ n = 81$)

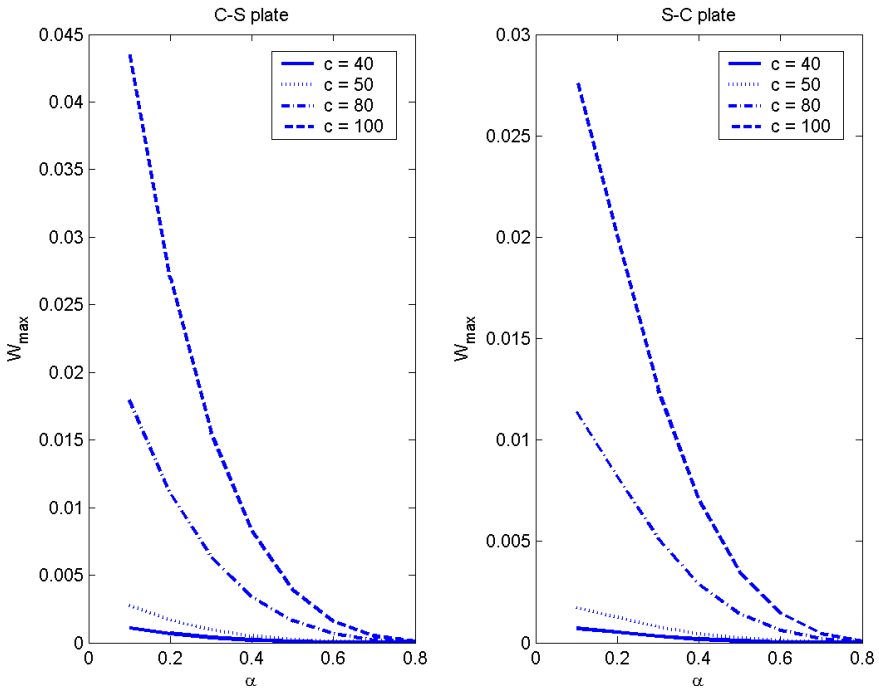

Figure 1: Change of W_{max} with respect to α

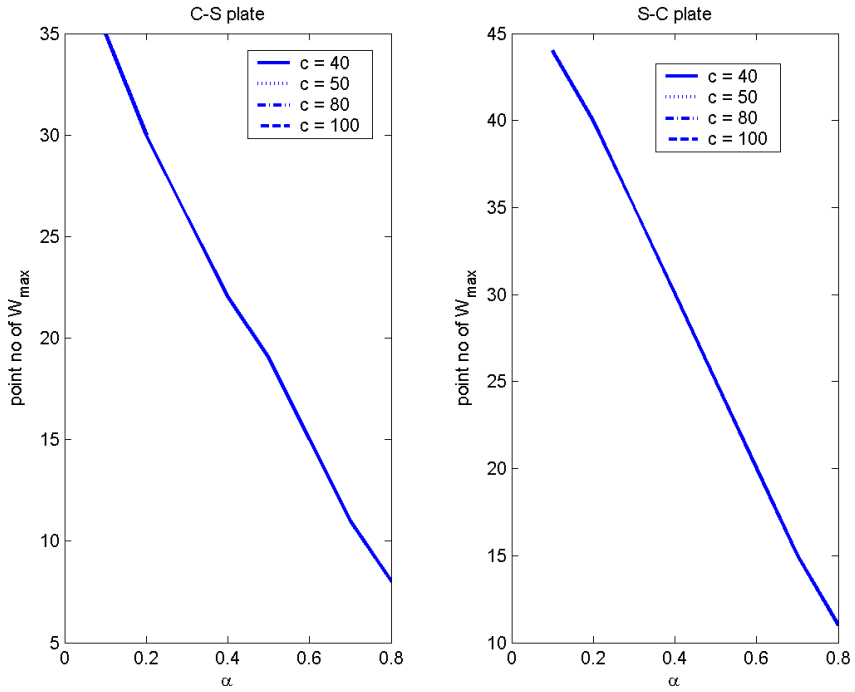

Figure 2: Location of W_{max} with respect to α

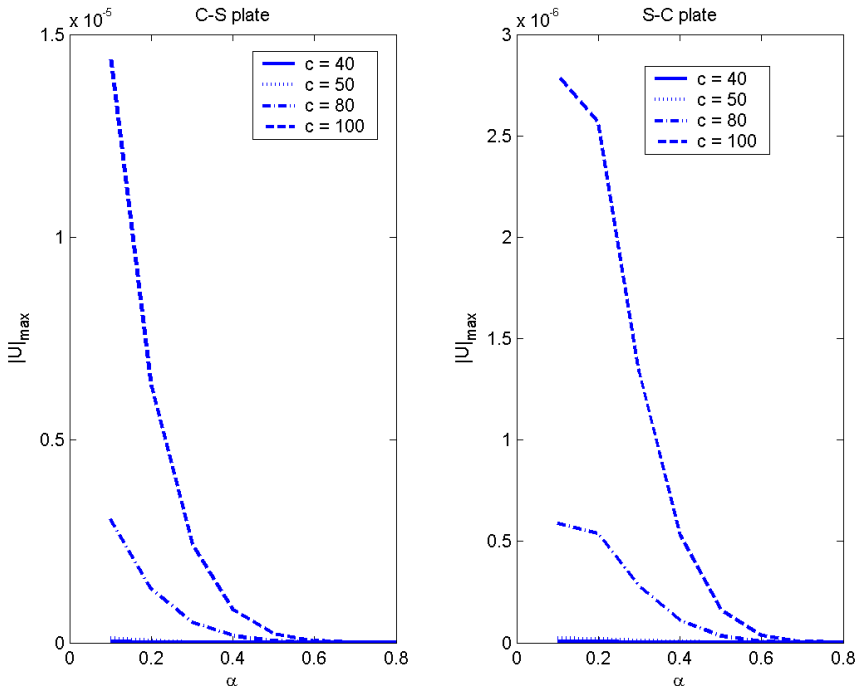

Figure 3: Change of $|U|_{\max}$ with respect to α

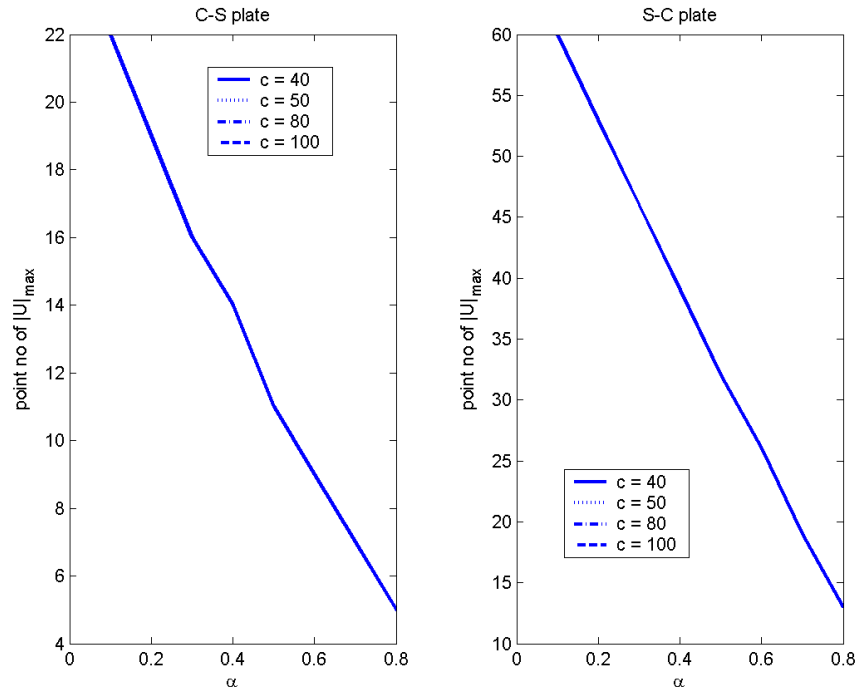

Figure 4: Location of $|U|_{\max}$ with respect to α

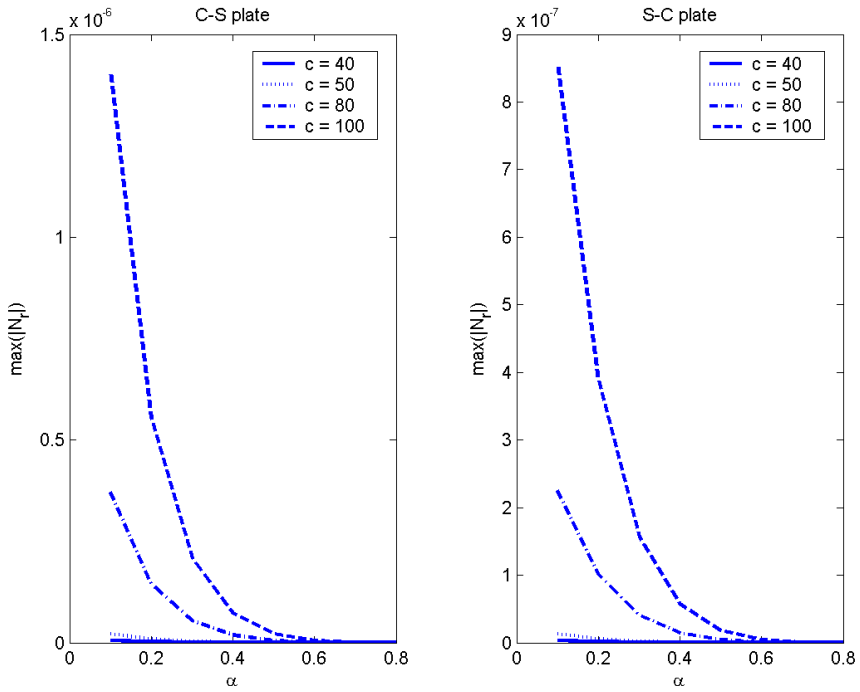

Figure 5: Change of $\max\left(\left|N_r\right|\right)$ with respect to α

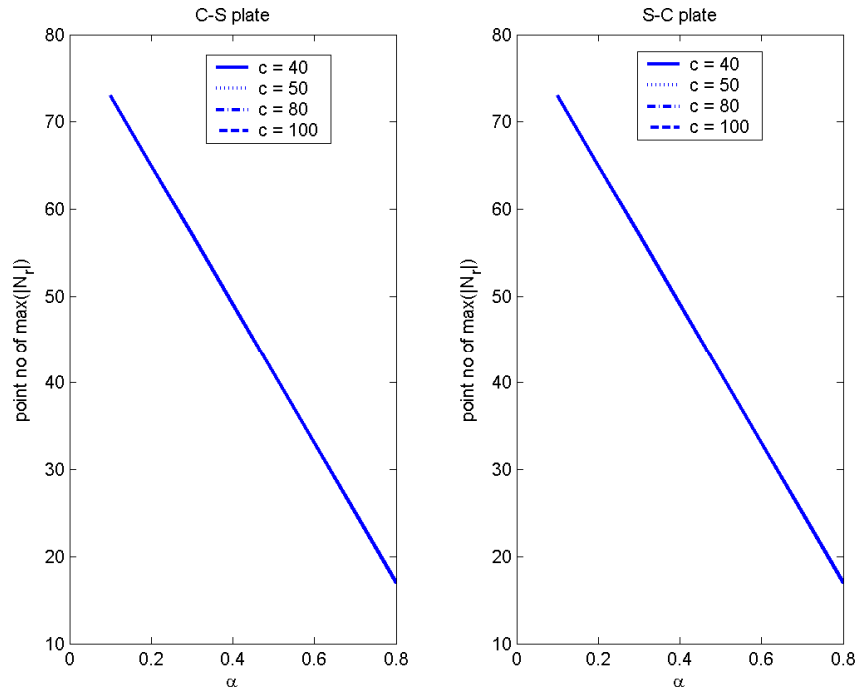

Figure 6: Location of $\max\left(\left|N_r\right|\right)$ with respect to α

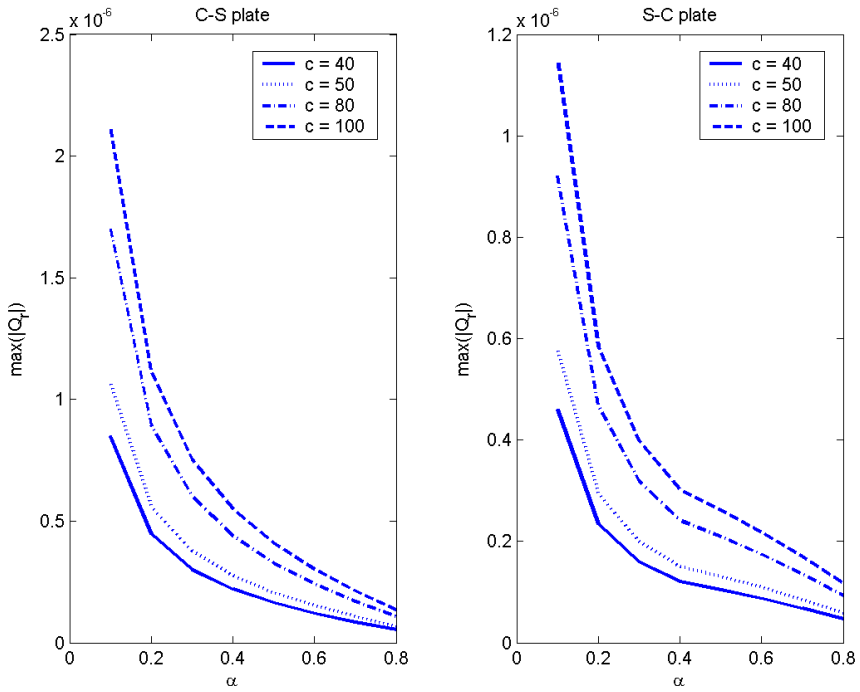

Figure 7: Change of $\max\left(|Q_r|\right)$ with respect to α

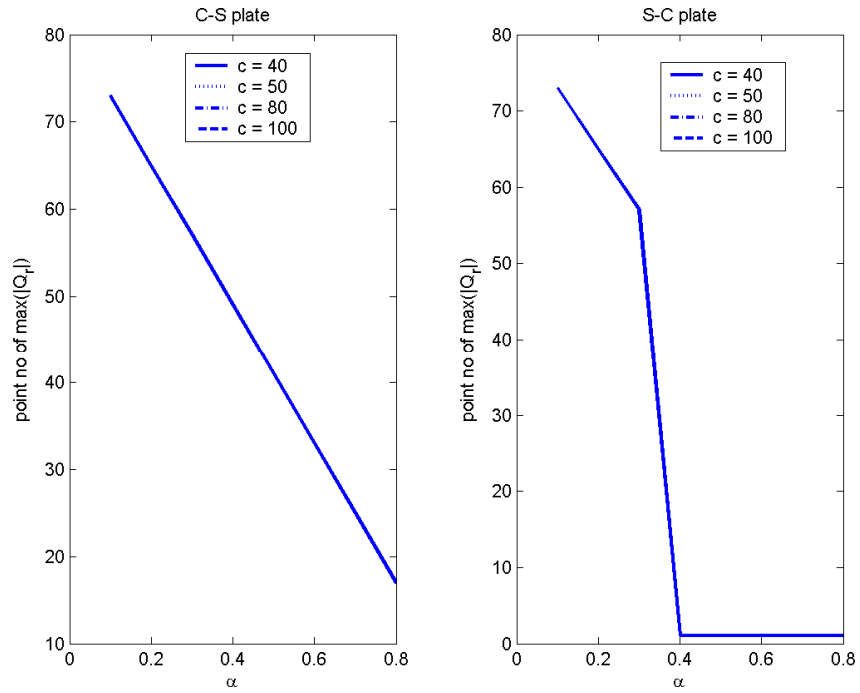

Figure 8: Location of $\max\left(|Q_r|\right)$ with respect to α

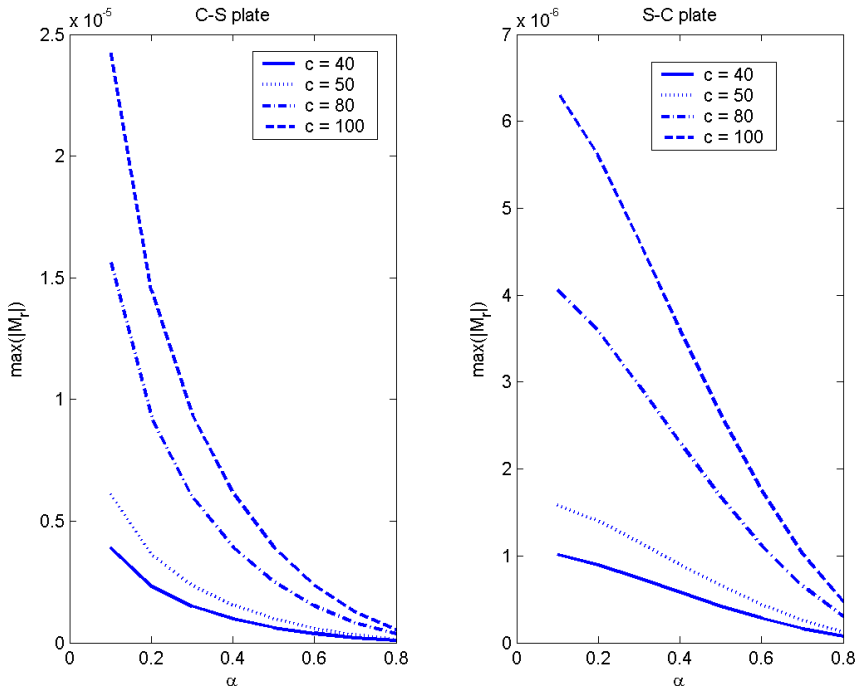

Figure 9: Change of $\max\left(\left|M_r\right|\right)$ with respect to α

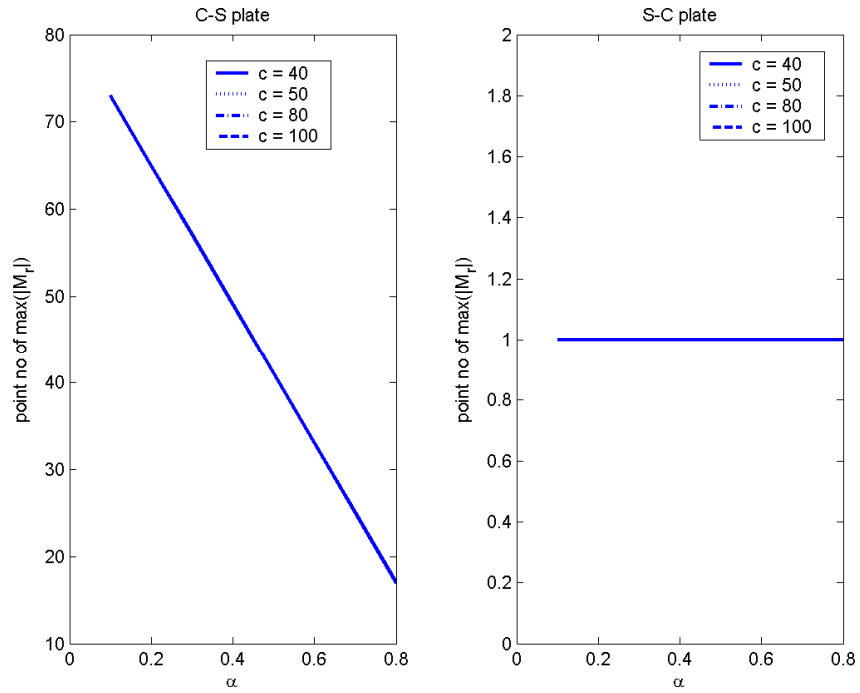

Figure 10: Location of $\max\left(\left|M_r\right|\right)$ with respect to α

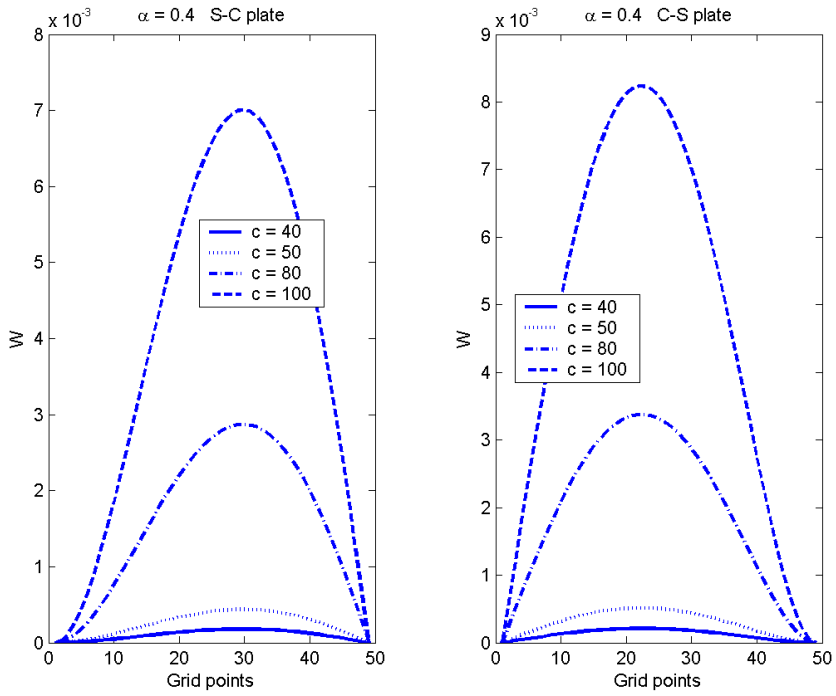

Figure 11: Influence of c on *W*

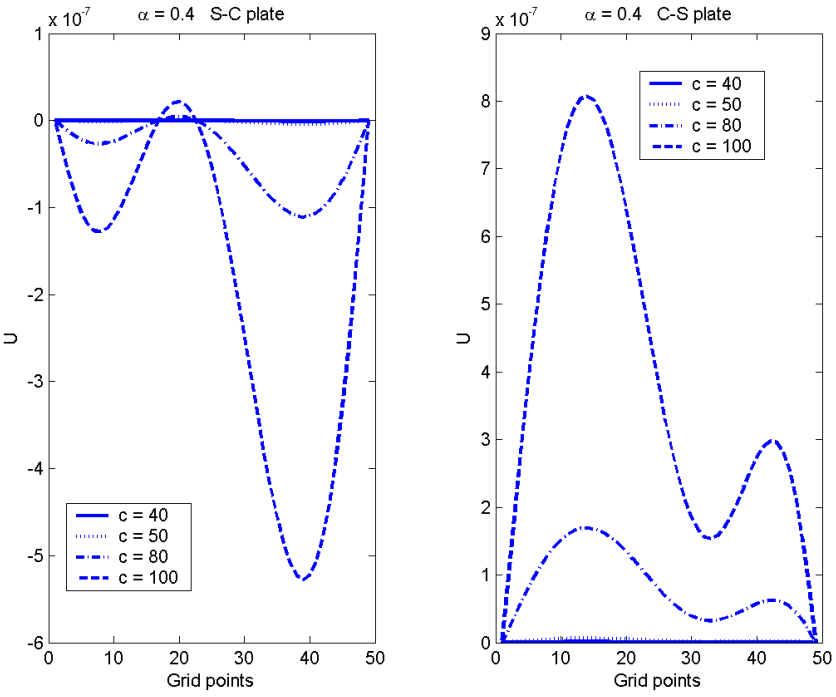

Figure 12: Influence of c on *U*

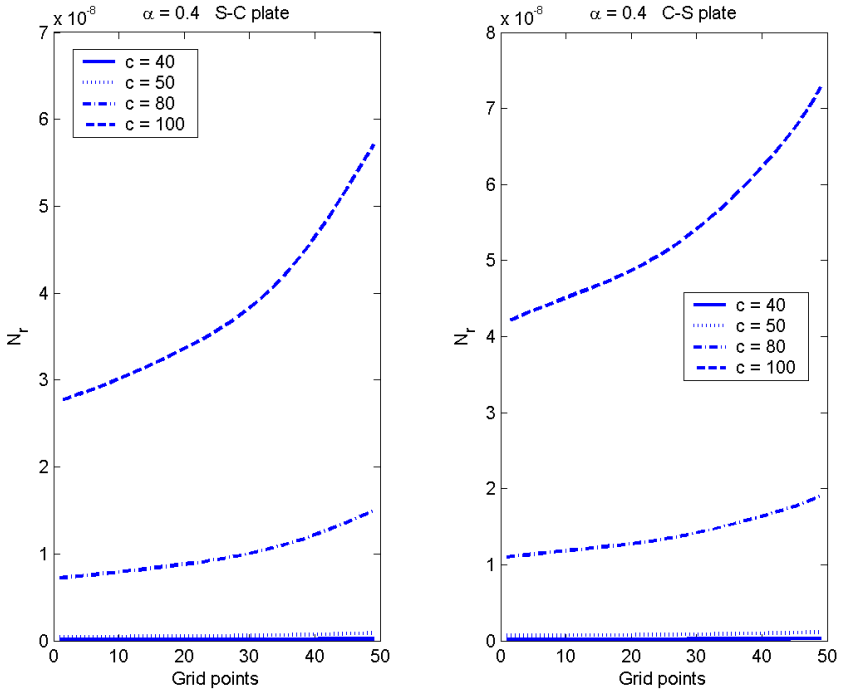

Figure 13: Influence of c on N_r

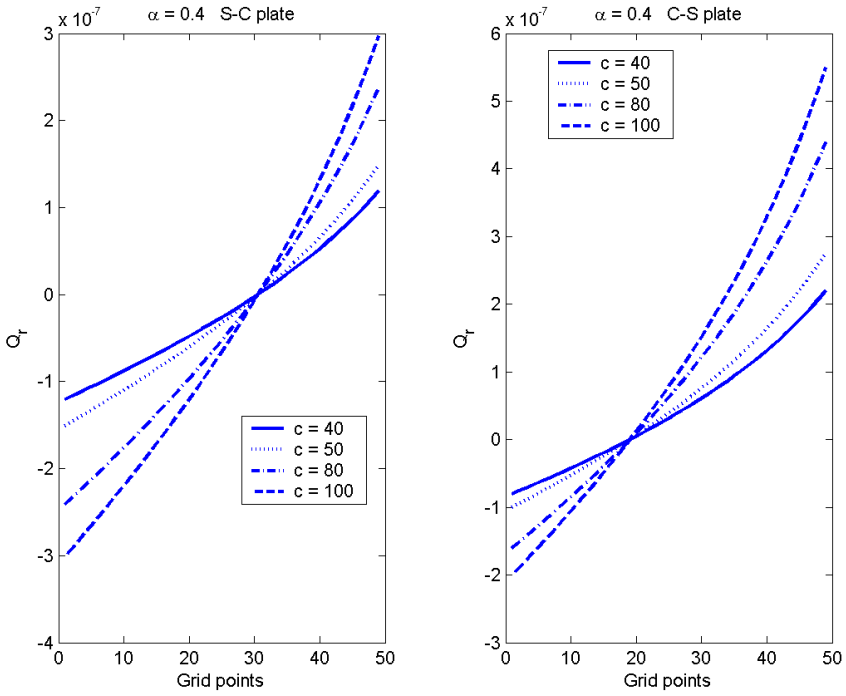

Figure 14: Influence of c on Q_r

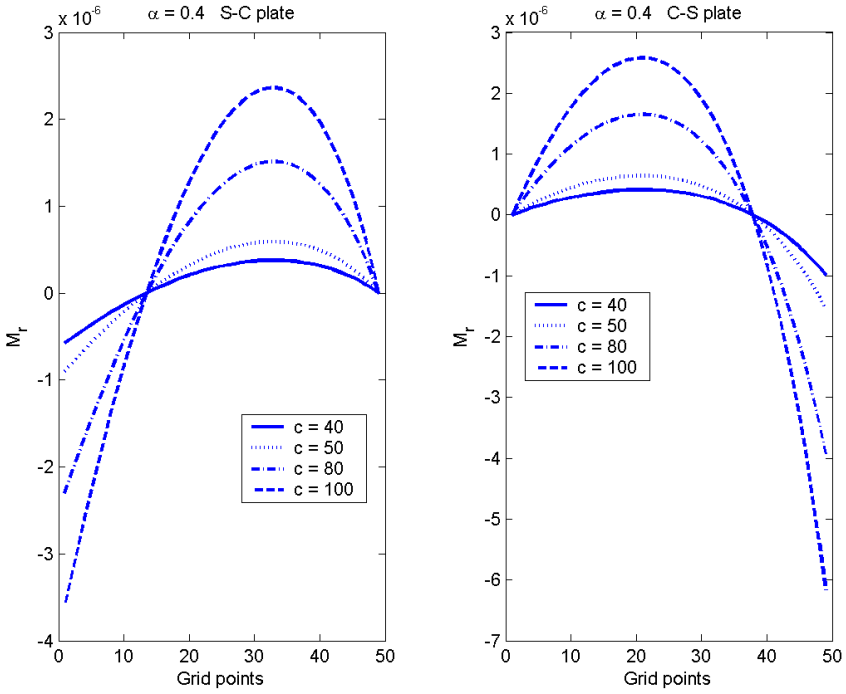

Figure 15: Influence of c on M_r

4 Concluding Remarks

The solutions made for $Q = 1\times10^{-8}$ covering S-C and C-S plates reveal that the parameter of thickness has dominant influence on the results (Figures 1-15). The main findings of the numerical results based on sensitivity analysis are outlined as follows:

- As the parameter of thickness is increased, or as the parameter of hole is decreased the maximum deflection increases (Figure 1).
- The location of the grid point where the maximum deflection develops is independent of the parameter of thickness (Figure 2).
- As the parameter of thickness is increased, or as the parameter of hole is decreased, the maximum value of the radial displacement increases (Figure 3).
- The location of the grid point which maximizes the radial displacement is independent of the parameter of thickness (Figure 4).
- As the parameter of thickness is increased, or as the parameter of hole is decreased $\max\left(\left|N_r\right|\right)$ increases (Figure 5).
- The location of the grid point where $\max\left(\left|N_r\right|\right)$ develops is independent of the parameter of thickness (Figure 6).

- As the parameter of thickness is increased, or as the parameter of hole is decreased $\max\left(\left|Q_r\right|\right)$ increases (Figure 7).
- The location of the grid point where $\max\left(\left|Q_r\right|\right)$ develops is independent of the parameter of thickness (Figure 8).
- As the parameter of thickness is increased, or as the parameter of hole is decreased $\max\left(\left|M_r\right|\right)$ increases. (Figure 9).
- The location of the grid point where $\max\left(\left|M_r\right|\right)$ develops is independent of the parameter of thickness (Figure 10).
- The parameter of thickness has dominant influence on the deflection (Figure 11).
- C-S plate produces larger deflection, radial displacement and membrane force than S-C plate does (Figures 11-13).
- For S-C plate when $\alpha \geq 0.4$ $\max\left(\left|Q_r\right|\right)$ develops at the outer edge (Figure 8).
- For S-C plate $\max\left(\left|M_r\right|\right)$ develops at the outer edge (Figure 10).

The algorithm used in the paper works efficiently and produces results with acceptable accuracy.

References

[1] N.C. Huang, "Unsymmetrical buckling of thin shallow spherical shells", Journal of Applied Mechanics-ASME, 31 (3), 447-457, 1964.

[2] M Altekin, R.F. Yükseler, "Large deflection analysis of clamped circular plates", WCE 2011 Proceedings, Volume III, IAENG, 6-8 July, 2011, London, U.K., 2210-2212.

[3] L.S. Ramachandra, D. Roy, "A novel technique in the solution of axisymmetric large deflection analysis of a circular plate", Journal of Applied Mechanics-ASME, 68 (5), 814-816, 2001.

[4] Q.S. Li, J. Liu, H.B. Xiao, "A new approach for bending analysis of thin circular plates with large deflection", International Journal of Mechanical Sciences, 46 (2), 173-180, 2004.

[5] R. Szilard, Theory and Analysis of Plates, Englewood Cliffs: Prentice-Hall Inc., 1974.

[6] S Timoshenko, S. Woinowsky-Krieger, Theories of Plates and Shells, New York: McGraw-Hill Book Company, 1959.

[7] C.M. Wang, "Relationships between Mindlin and Kirchhoff bending solutions for tapered circular and annular plates", Engineering Structures, 19 (3), 255-258, 1997.

[8] J.B. Han, K.M. Liew, "Analysis of annular Reissner/Mindlin plates using differential quadrature method", International Journal of Mechanical Sciences, 40 (7), 651-661, 1998.